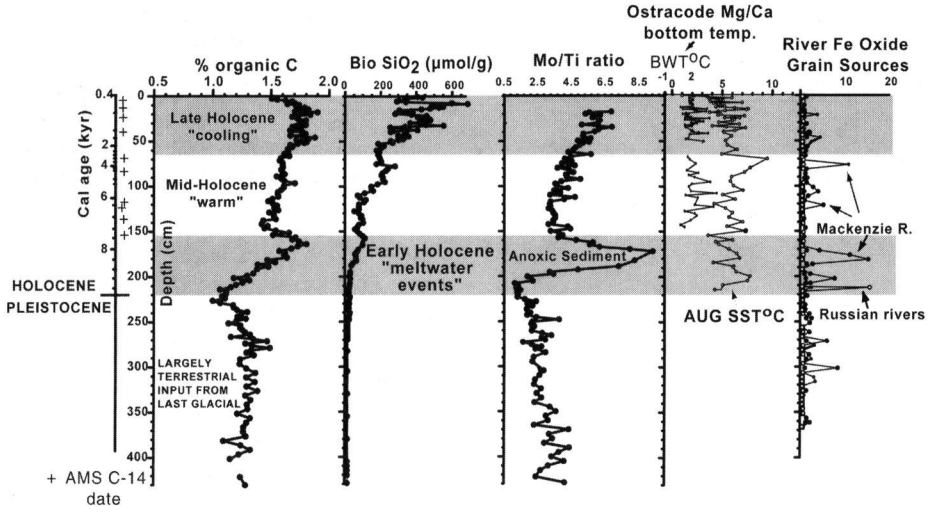

Fig. 3. Percent organic C, biogenic Si, and Mo/Ti in the bulk sediment of P1 and B3 are compared to August sea surface temperature (SST), bottom water temperature (BWT), and to the Fe oxide grains from the Mackenzie River (northern Canada) and the Russian rivers (Ob and Yenisey). The SST, based on a dinocyst transfer function, and the BWT, based on Mg/Ca in the ostracode, Krithe glacialis, *show rapid fluctuations and much warmer conditions during most of the Holocene as compared to today. The error on the SST values is ±1.8°C and most fluctuations are greater than this error. The lowermost shaded interval is a time of abundant meltwater and includes an anoxic sediment interval corresponding to the Mo/Ti peak. The upper shaded interval is a time of general cooling and the interval between is the mid-Holocene warm period. Sampling interval in B3 is 1 cm (~45 years) and in P1, 5 cm (~225 years).*

5°C and was 3–7°C warmer than it is today (Figure 3). This magnitude of change is analogous to the polar front shifting more than 20° in latitude from its current location near the Aleutian Islands (50°N) to just north of Barrow, Alaska.

Benthic calcareous microfossils—foraminifers and ostracodes—only appear after the early Holocene, but they show significant fluctuations in abundance and species diversity, such that the middle and late Holocene can be subdivided into five benthic faunal zones (see Web site). While the specific environmental changes that led to the Holocene benthic faunal shifts will remain enigmatic until further modern faunal analog studies are undertaken, the P1 faunal record clearly demonstrates that bottom water conditions varied considerably during the Holocene. This contention is corroborated by the P1 record of bottom water temperature (BWT) reconstructed from Mg/Ca ratios of ostracode shells (Figure 3). This record indicates rapid and large (1–2°C) shifts in BWT superimposed on a net cooling of around 1°C since the mid-Holocene.

The variability in the benthic water proxies is not surprising given that the P1 site lies near the sharp hydrographic boundary between the cold, fresh surface waters and the relatively warm, saline waters of the Atlantic Intermediate layer. The observed BWT oscillations at P1 possibly resulted from fluctuations in the extent or temperature of the Atlantic layer. The warm pulses are perhaps analogous to the recent warming detected in the Atlantic layer driven by stronger Atlantic inflow, which, in turn, has been attributed to an enhanced positive phase of the Arctic/North Atlantic Oscillation [e.g., *Swift et al.*, 1997].

Thus, the surface circulation and possibly the extent of the Atlantic-derived intermediate water appear to have changed several times during the Holocene. Our records indicate that Holocene variability in the western Arctic is larger than any change observed in this area over the last century. While recently observed polar warming is dramatic, the record of change in core P1 suggests that mid-Holocene temperatures may have been 5°C warmer only a few thousand years ago. In this respect, future work should be focused on higher resolution climate records from the Arctic Ocean. The study of P1 provides encouragement that even higher resolution records can be recovered from the upper continental slopes of this ocean.

Authors

D. Darby, J. Bischof, G. Cutter, A. de Vernal, C. Hillaire-Marcel, G. Dwyer, J. McManus, L. Osterman, L. Polyak, and R. Poore
For additional information, contact D. Darby, Department of Ocean, Earth, & Atmospheric Sciences, Old Dominion University, Norfolk, Va., USA; E-mail: ddarby@odu.edu.

References

Darby, D. A., and J. F. Bischof, A statistical approach to source determination of lithic and Fe-oxide grains: An example from the Alpha Ridge, Arctic Ocean, *J. Sediment. Res., 66*, 599–607, 1996.

Duplessy, J. C., E. Ivanova, I. Murdmaa, M. Paterne, and L. Labeyrie, Holocene paleoceanography of the northern Barents Sea and variations of the northward heat transport of the Atlantic Ocean, *Boreas, 30*, 2–16, 2001.

PARCS, *The Arctic Paleosciences in the Context of Global Change Research-PARCS*, Paleoenvironmental Arctic Sciences, ESH Secretariat, 95 pp., AGU, Washington, D.C., 1999.

Proshutinsky, A., and M. Johnson, Two circulation regimes of the wind driven Arctic Ocean, *J. Geophys. Res., 102*, 12,493–12,514, 1997.

Stein, R., Circum-Arctic river discharge and its geological record: An introduction, *Int. J. Earth Sci., 89*, 447–449, 2000.

Swift, J. H., E. P. Jones, K. Aagarard, E. C. Carmack, M. Hingston, R. W. Macdonald, F. A. Mclaughlin, and R. G. Perkin, Waters of the Makarov and Canada basins, *Deep-Sea Res. II, 44*, 1503–1529, 1997.

Thompson, D. W. J., and J. M. Wallace, The Arctic Oscillation signature in the wintertime geopotential height and temperature fields, *Geophys. Res. Lett., 25*, 1297–1300, 1998.

Imaging Spectroscopy Measures Desertification in United States and Argentina

PAGES 601, 605–606

Much international environmental research and policy development now focuses on desertification in arid and semi-arid ecosystems of the world. These "dryland" regions, which include most of the world's shrublands, grasslands, and savannas, cover nearly 45% of the Earth's land surface and support a large fraction of the world's food production. The U.S. Senate, along with 173 other countries, recently ratified the United Nations (U.N.) Convention to Combat Desertification [*UNEP*, 1992], a multinational effort to address this pressing human and environmental problem [*Showstack*, 2001].

The U.N. describes desertification as "land degradation in arid, semi-arid and dry subhumid areas (drylands) resulting mainly from adverse human impact. It is a widespread but discrete spatial process of land degradation throughout the drylands that is quite different from the phenomenon of observed cyclic oscillations of vegetation productivity at desert fringes ('desert expansion or contraction') as revealed by satellite data and related to climate fluctuations. At present desertification directly affects about 3.6 billion hectares—70% of the total drylands, or nearly one quarter of the total land area of the

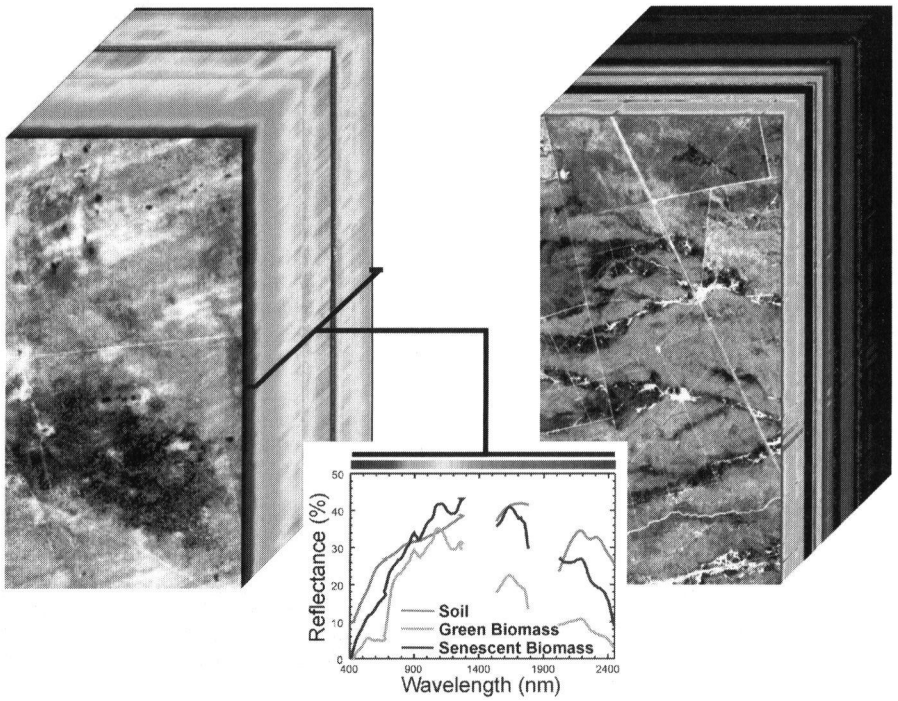

Fig. 1. Imaging spectrometers gather upwelling Earth radiance information in three-dimensional data "cubes," such as in this NASA Airborne Visible and Infrared Imaging Spectrometer (AVIRIS) image of the Jornada LTER arid land research site in New Mexico (left), and this EO-1 Hyperion image of the Ñacuñán Biosphere Reserve, central Argentina (right). The images contain a third spectroscopic dimension that provides quantitative information on the physical and chemical properties of live and senescent vegetation and soils. Example spectra of surface materials demonstrating this third dimension are shown in the graph inset. Original color image appears at the back of this volume.

world, and about one sixth of the world's population." [*UNEP*, 1992].

Scientists and policy-makers recognize that quantitative, regional-scale assessment and monitoring of drylands is critically needed to assess patterns and causes of ecological change in these regions. Meeting this goal has remained a challenge due to the spatial complexity of arid and semi-arid landscapes. This spatial complexity results in reflected light properties that have a dimensionality exceeding the capabilities of existing space-borne remote sensing instruments. However, new advances in a unique form of remote sensing, called imaging spectroscopy, are providing the needed biogeophysical information to measure and monitor dryland regions from remote vantage points.

Imaging spectroscopy, or hyperspectral imaging, is the measurement of solar radiation reflected from the Earth's surface in contiguous, narrow spectral channels, usually spanning the wavelength region from 0.4 μm to 2.5 μm. The measurements are collected as three-dimensional data "cubes" that have two spatial and one spectral dimension (Figure 1). These data cubes can be thought of as stacks of images with each image representing the light reflected from a narrow wavelength region, or as assemblages of spectra where a reflected light spectrum is measured for each point in the image. In these data, the spectra record the molecular absorption and constituent scattering effects of the surface. The high dimensionality (> 200 spectral channels) can allow identification of materials with overlapping, but distinct, spectral signatures. It is the spectroscopic dimension of these data that allows the chemical and physical properties of the imaged materials to be quantitatively determined.

These spectroscopic imaging signatures, in conjunction with new land surface radiation models, can be used to accurately determine the physical and chemical properties of dryland regions. Furthermore, remote imaging spectroscopy allows regions to be examined over spatial scales ranging from tens of square meters to thousands of square kilometers. Imaging spectroscopy measurements of vegetation characteristics, such as vegetation type, canopy cover and water content, foliage biomass, senescent vegetation, and bare soil properties can now determine the geographic extent and biophysical condition of degraded lands. In doing so, imaging spectroscopy is providing access to a range of dryland ecosystem properties that were formerly inaccessible using traditional remote sensing instruments or ground-based studies.

Land Degradation and Desertification in Dryland Regions

Relative to other ecosystems, arid and semi-arid regions are disproportionately prone to ecological damage from land use. Cattle ranching is a dominant activity in these regions [*FAO*, 1997]. Although agricultural land use is not as extensive as grazing, it leads to a complete modification of dryland ecosystems and biogeochemical processes. Climate variability plays an important role in land use and contributes to ecological change in these regions. However, land use is the clear dominant factor in the degradation of dryland ecosystems, with documented losses in natural vegetation cover, shifts in plant function and structure, changes in water and nutrient cycles, and desertification [e.g., *Schlesinger et al.*, 1990].

Many local-scale studies have documented the effects of land use in dryland ecosystems. However, we still lack quantitative information on the vegetation and biogeochemical changes associated with regional land-use policies in these regions. UNEP [1992] also notes: "Assessment of the current global status of desertification/land degradation has shown that accurate hard data, which would allow it to be stated with some preciseness to which degree and with what rate desertification is taking place in various parts of the world, are still lacking." This statement resonates with the current level of uncertainty in most land-use change and climate impact studies of dryland regions.

Ideally, traditional remote sensing would be a key contributor to understanding these issues, but progress toward an operational capability for quantifying land surface changes specific to desertification has been hindered by the high spectral dimensionality of the surface signatures. Does imaging spectroscopy provide a new viable strategy?

The answer to this question lies in understanding the type of Earth surface information needed to resolve the biogeophysical conditions indicating the overuse, degradation, or desertification of drylands. For example, heavy cattle grazing can result in a temporally and spatially persistent decrease in live grassland biomass and surface dry litter. It can also favor the replacement of grasslands with woody plant species that do not provide cattle forage. Constant removal of dryland vegetation also disrupts biogeochemically important processes such as nutrient cycling and surface energy balance. In a long-term overgrazing scenario, an ecosystem that has shifted from grassland dominance to shrub-soil system cannot support cattle grazing practices. Nor can this system easily return to the prior grassland ecosystem due to the re-allocation of nutrients and biological resources.

This scenario and others like it show that remote sensing-based monitoring of land degradation and desertification requires measurements of both live and senescent vegetation extent and condition, as well as bare soil areas, over large regions. Changes in the spatial aggregation of these materials must be resolved. Multi-spectral remote sensing observations with limited spectral sampling have not reliably provided this information, but imaging spectroscopy with full solar-reflected spectral signatures is now doing so from airborne and space-based observations.

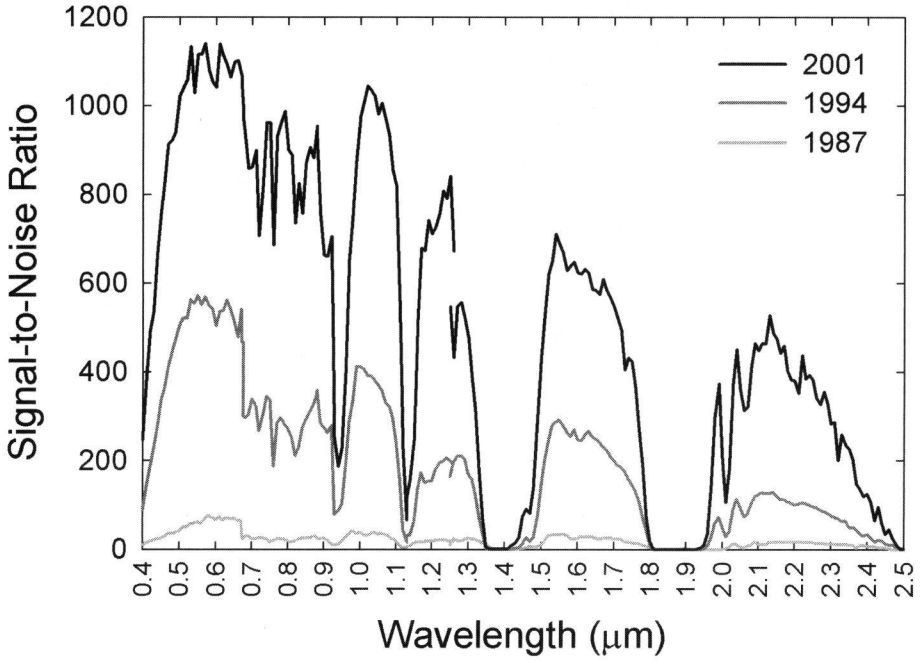

Fig. 2. The signal-to-noise performance of the NASA AVIRIS instrument has increased dramatically in the last 15 years, allowing measurements today that were not previously obtainable from airborne vantage points.

High-performance Airborne Imaging Spectroscopy

In the past few decades, imaging spectroscopy has dramatically evolved in its ability to deliver spectral reflectance measurements of the Earth with precision and accuracy previously obtainable only in a laboratory setting. The NASA Airborne Visible and Infrared Imaging Spectrometer (AVIRIS) [*Green et al.*, 1998], which was developed by the Jet Propulsion Laboratory, is currently the highest performance instrument of this kind.

AVIRIS collects measurements in 224 channels spanning the 0.37–2.5 μm wavelength range. It is flown at high altitude (~20 km) aboard a NASA ER-2 aircraft or at low altitude (~4 km) aboard a Twin Otter, which yields a spatial resolution of 20 m and 4 m, respectively. AVIRIS data are spectrally, radiometrically, and spatially calibrated. Driven by science requirements, the signal-to-noise performance of AVIRIS has been improved significantly over the years (Figure 2), providing scientists with the new measurements needed to study the physical and chemical properties of land surface materials.

Using recent AVIRIS data sets, studies of dryland ecosystems, land degradation, and desertification are underway in the southwestern United States and central Argentina. The goals of this effort are to improve understanding of the physical and biogeochemical impacts of human activities as well as the role of climate variability in these regions. An essential element of these studies is determination of the spatial pattern and aboveground biomass distribution of live and senescent vegetation and bare soils from imaging spectroscopy data.

Spectroscopy of Degraded Lands in the United States

One of the study regions includes the National Science Foundation Jornada Long-term Ecological Research (LTER) site, located in southern New Mexico (Figure 1). The area has a well-documented history relating grazing management and drought to observed processes of desertification (see www://jornada.nmsu.edu). Ecological conditions accompanying desertification include the replacement of ecosystems containing relatively homogeneous stretches of live and senescent grassland biomass with shrublands comprised of spatially aggregated woody plant clusters embedded in a matrix of nearly bare soil. The biogeochemical consequences of this transformation have been intensively studied [e.g., *Schlesinger et al.*, 1990].

For the past few decades, vegetation greenness maps of the Southwest United States, including the Jornada LTER site, have been constructed using visible and near-infrared wavelength channels from multi-spectral sensors. However, vegetation greenness does not easily depict the location and extent of degraded lands. Greenness is often temporally and spatially variable due to the dominance of locally convective precipitation in arid regions. In addition, the vegetation leaf biomass and seasonal variability of shrublands and grasslands are often not revealed in multi- spectral satellite observations, especially in areas where the two vegetation types intimately occur together. Even the highest spatial resolution sensors, such as aerial photographs from low-altitude aircraft, cannot well quantify the small changes in vegetation biophysical properties that best indicate the onset or progression of desertification in pastoral ecosystems.

High-performance imaging spectroscopy, such as from the AVIRIS sensor, does provide the observations required for quantitative studies of land degradation in these spatially complex dryland ecosystems. The measurements provide two specific capabilities for applications in desertification research. First, high spectral resolution visible, near-infrared, and shortwave-infrared (0.4–2.5 μm) observations provide a means to identify the presence of live and senescent vegetation canopies. Properties of these canopies derived from the spectroscopic measurements include leaf area index, water content, and aboveground live and senescent biomass. Second, the spectroscopic observations allow accurate measurement of vegetation and bare soil extent at the sub-pixel scale, resulting in continuous spatial fields of these surface properties. This suite of information opens the door for new quantitative studies of ecosystem responses to land use and climate variability in dryland regions.

New algorithms and physical models of the land surface that utilize the unique information contained in spectroscopic data cubes are needed to obtain the precise amount and spatial pattern of live vegetation, surface litter, and bare soils [*Asner et al.*, 1998; *Asner and Lobell*, 2000]. The methods are often computationally expensive but are now highly automated and capitalize on efficient, parallel-processor "Beowulf" computers (for more, see http://sdcd.gsfc.nasa.gov).

At the Jornada LTER site, the most distinct grassland and shrubland ecosystems are readily apparent on the ground and even in traditional multi-spectral satellite imagery. However, spatial transitions from grassland and shrubland ecosystems are much more challenging from either field- or remote sensing-based vantage points. Measurement of the transition zones is critically important for understanding not only rates of land-cover change but also the human and ecological drivers of desertification. The ecology and biogeochemistry of desertification itself cannot be well studied without such measurements in the transition zones.

Figure 3a is a typical illustration of changes in the biogeophysical characteristics of the land surface across these desertification transition zones. AVIRIS spectroscopic observations were analyzed using a physical model of the land surface [*Asner et al.*, 1998]. Full spectral signatures were required for this analysis in the context of the large spectral/compositional variability present in these ecosystems. The resulting image depicts the spatial extent and pattern of live vegetation (red), surface litter (green), and bare soils (blue) at the sub-pixel scale or on a spatially contiguous basis. This spectroscopic analysis shows the grassland and shrubland areas with clarity, a result that has not been fully available from other imaging systems. More important, the fine spatial structure of vegetation and soil cover is well quantified throughout the transition zone between grassland and shrubland areas.

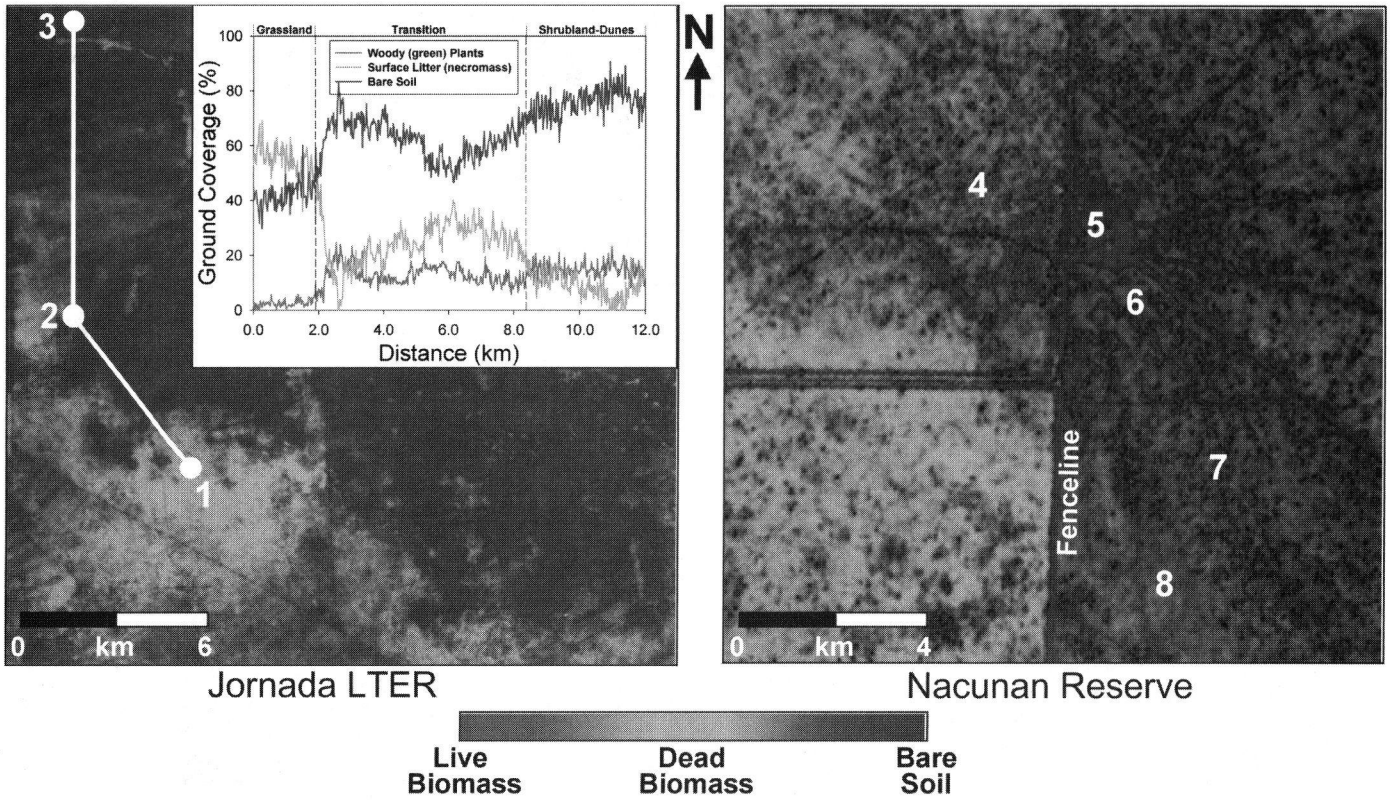

Fig. 3. AVIRIS imagery of the Jornada LTER site (a) and the Ñacuñán Biosphere Reserve (b) is interpreted using physical-spectroscopic models of the land surface. These models are used to estimate fractional cover and biomass of live vegetation and senescent plant materials as well as bare soil cover and geochemistry. The Jornada image contains grasslands (1) that have been converted to shrublands (3) as well as large expanses of transition zone (2) through documented processes of land degradation and desertification. The Ñacuñán image shows the reserve to the left of the center fence line containing areas of mixed live and senescent vegetation with little bare soil (4). To the right of the fence, a cattle ranch (5) is surrounded by thick green, woody vegetation (6) that transitions into areas of low senescent biomass (7) and further to regions of high bare soil cover (8). Original color image appears at the back of this volume.

The graph inset of Figure 3a shows the live vegetation and bare soil ground cover along a transect crossing from the grassland through the transition zone and into the shrubland. While bare soil cover quickly increases and surface litter decreases outside of the grassland region, the transition zone contains larger amounts of surface litter and less bare soil than the shrubland ecosystem. However, the fractional ground coverage of green plants in the transition zone and the shrubland is statistically similar. It is the spectroscopic measurement of the standing biomass of senescent and dead vegetation that allows accurate determination of the grassland to shrubland transition.

Although these observations of live and senescent biomass quantify the transition between two distinct ecosystems, they also depict varying surface conditions that represent important biogeochemical changes occurring in the region. Schlesinger et al. [1996] showed that the spatial distribution of soil nitrogen and phosphorus stocks was homogeneously distributed throughout the grassland ecosystems, but spatially aggregated under woody plant clusters in the shrubland region. Our studies indicate that nutrient and carbon stocks are aggregated spatially in the transition zone, more so than in the grassland areas but less so than in the shrubland systems. Thus, the spatial patterning of live vegetation and surface litter is correlated with sub-surface processing of biologically important nutrients. Reliable quantification of these surface constituents provides a window into the biogeochemistry of a changing landscape, a capability that only became operational in the late 1990s using advanced imaging spectrometers with very high signal-to-noise performance (Figure 2).

Spectroscopy of Degraded Lands in Argentina

Contrasting with the New Mexico site is a dryland region of central Argentina, where heavy grazing has resulted in another form of desertification described by Ojeda et al. [1998] (see http://www.cricyt.edu.ar). Spectroscopic analysis of AVIRIS data measured in January 2001 indicate areas of land degradation characterized by patterns of vegetation change previously described in Australian rangelands [e.g., *Pickup and Chewings*, 1994].

Figure 3b shows part of the Ñacuñán Biosphere Reserve, located in the Monte Desert to the southeast of the city of Mendoza. An interior section of the reserve is located to the left of the north-south-oriented fence. Ecosystems within the reserve are characterized by woody plant clusters (red) embedded in a matrix of live and senescent grassland cover (green). In this part of the reserve, the only areas of significant bare soil are roads and trails. To the right of the fence is a cattle ranch known locally for its intense grazing management practices. The spectroscopic observations indicate that the ranch and immediate surroundings are denuded of live or senescent vegetation, leaving only bare soil. In an arc around the ranch is a region of thick woody vegetation containing significant leaf biomass (red). This arc of woody vegetation has likely resulted from seed deposition by cattle, local fire suppression, and other management conditions favoring woody plant establishment. Farther away from the locus of ranching operations, the landscape changes again to scattered green, woody plants of a spatial density very similar to the areas within the neighboring reserve. However, dramatically less senescent grassland cover is found in these primary grazing regions outside of the reserve, as is indicated by blue tones in the image data.

A persistent lack of grassland vegetation outside of the Ñacuñán Biosphere Reserve is a clear result of heavy grazing land use practices. Field studies show a disruption of biogeochemical processes in these areas, such as loss of biologically important soil nutrients and carbon stocks. These measured changes are a critical indicator of land degradation. Long-term, operational monitoring of these surface conditions would indicate the onset of desertification if, for example, grassland vegetation biomass remained low while woody plant biomass increased. Such change

would resemble the spatial patterns of live vegetation, surface litter, and bare soils found at the Jornada site in New Mexico.

Spaceborne Imaging Spectrometers: Now and the Future

November 22, 2000, marked the launch of the first Earth-looking spaceborne imaging spectrometer. The NASA Earth Observing-1 satellite carries the Hyperion instrument onboard, providing the first space-based hyperspectral observations of terrestrial ecosystems worldwide. Hyperion collects measurements of reflected radiance in 220 spectral bands covering the 0.4–2.5 μm wavelength region of the spectrum and has a spatial resolution of 30 m.

The EO-1 Hyperion instrument is currently collecting data over the Jornada, Ñacuñán, and many other dryland sites throughout the world. The spectroscopic data are undergoing rigorous evaluation, often using AVIRIS as a comparison, to derive the ecosystem properties summarized above and other land-surface characteristics. One of the first Hyperion images collected during the EO-1 mission is shown in Figure 1, depicting part of the Ñacuñán Biosphere Reserve in central Argentina.

EO-1 Hyperion is a technology demonstration and is not deployed for general operational use. A primary goal of the EO-1 program will be to provide technical and scientific input to future orbital imaging spectrometer missions. In this way, the combination of AVIRIS and Hyperion is demonstrating the use of imaging spectroscopy for measuring and monitoring critical aspects of dryland ecosystems for global change research and applications.

Today, Hyperion is the only Earth orbiting imaging spectrometer. The U.S. Air Force is developing the Warfighter imaging spectrometer, which will provide Earth scientists with some access to ecosystem observations. Hyperion and Warfighter serve as major first steps to placing a spectroscopic measurement capability in orbit. However, their performance is less than that achieved by an AVIRIS-class, high-performance imaging spectrometers.

The studies summarized here, as well as many others occurring around the world, emphasize the value and need for operational high performance imaging spectrometer observations of the Earth's land ecosystems. The science community that uses imaging spectroscopy data has established requirements for instruments with high signal-to-noise ratios, uniformity, and calibration accuracy. Future spaceborne spectrometer programs will need to achieve these higher levels of performance to accurately measure the surface composition, biogeophysical, and chemical properties of ecosystems with global sampling over large spatial scales. This new class of spectroscopic measurements will revolutionize Earth system studies ranging from the terrestrial carbon cycle and land-use change, to ecosystem dynamics and biogeochemical cycles.

Acknowledgments

We thank K. Heidebrecht, B. Sawtelle, B. Constance, S. Parks, B. Nolen, A. Huete, C. Borghi, S. Tabeni, and R. Ojeda for their participation in these studies. This work is supported by NASA NIP grant NAG5-8709 and NASA NMP (EO-1) grant NCC5-480.

A portion of this work was carried out at the Jet Propulsion Laboratory/California Institute of Technology, Pasadena, California, under contract with NASA.

Authors

Gregory P. Asner, Department of Geological Sciences and Environmental Studies Program, University of Colorado, Boulder, USA; and *Robert O. Green*, Jet Propulsion Laboratory, Pasadena, Calif., USA

For additional information, contact Gregory P. Asner; E-mail: asner@colorado.edu

References

Asner, G. P., and D. B. Lobell, A biogeophysical approach for automated SWIR unmixing of soils and vegetation, *Rem. Sens. Environ., 74*, 99–112, 2000.

Asner, G. P., C. A. Wessman, and D. S. Schimel, Heterogeneity of savanna canopy structure and function from imaging spectrometry and inverse modeling, *Ecol. Applic., 8*, 1022–1036, 1998.

Food and Agriculture Organisation, *The State of Food and Agriculture*, FAO Agricultural Series 30, FAO, 1997.

Green, R. O., et al., Imaging spectroscopy and the Airborne Visible Infrared Imaging Spectrometer (AVIRIS), *Remote Sens. Environ. 65, 227–248, 1998.*

Ojeda, R. A., C. M. Campos, J. M. Gonnet, C. E. Borghi, and V. G. Roig, The MaB Reserve of Ñacuñán, Argentina: Its role in understanding the Monte Desert biome, *J. Arid Environ., 39*, 299–313, 1998.

Pickup, G., and V. H. Chewings, A grazing gradient approach to land degradation assessment in arid areas from remotely-sensed data, *Int. J. Remote Sens., 15*, 597–617, 1994.

Schlesinger, W. H., J. A. Raikes, and A. F. Cross, On the spatial pattern of soil nutrients in desert ecosystems, *Ecology, 77*, 364–374, 1996.

Schlesinger, W. H., J. F. Reynolds, G. L. Cunningham, L. F. Huenneke, W. M. Jarrell, R. A. Virginia, and W. G. Whitford, Biological feedbacks in global desertification, *Science, 247*, 1043–1048, 1990.

Showstack, R., Desertification treaty includes key role for scientists, *Eos, Trans. AGU, 82*, 298, 2001.

UNEP, *Status of Desertification and Implementation of the United Nations Plan of Action to Combat Desertification*, United Nations Environment Programme, Nairobi, Kenya, 1992.

Grouted Sediment Slices Show Signs of Earthquake Shaking

PAGES 603, 608

Sand and mud from Washington State, sampled with Japanese methods for identifying structure in unconsolidated deposits, have provided new evidence for earthquakes over the past 2000 years at the Cascadia subduction zone. Each sample was collected as a vertical slice, 0.5 m wide and up to 8 m long, in sheetpile driven into wet sand and mud beneath a tidal bank of the Columbia River (Figures 1 and 2). Painted with flexible, hydrophilic grout, the slices yielded full-size peels that reveal bedding and its disruption (Figure 3). Evidence for liquefaction is common, even where it is absent at the ground surface. Especially common are sills that imply lateral escape of water. These findings may affect ground-motion estimates for plate-boundary earthquakes in the northwestern United States and Canada.

The work began a 2-year project, supported by the government of Japan, to demonstrate geoslicers in the United States. Geoslicers were invented in Japan to reveal subsurface geology across active faults where digging space is narrow and ground is wet [*Nakata and Shimazaki*, 1997; *Haraguchi et al.*, 1998]. They have potential uses in other fields, such as groundwater hydrology, that focus on water-saturated deposits. In the rest of the demonstration project, geoslicers sampled lahar-runout sand in Seattle, the Hayward fault in California, and sand blows in Arkansas.

Geoslicers

A geoslicer consists of a sample tray and a shutter plate that are driven one at a time by a weighted vibrator. Driven first is the sample tray—in our case, a sheetpile—that has a broad back, a narrow flange on each of two sides, and no front, top, or bottom. The shutter plate, driven second, closes the front of the sample tray; as the plate descends, it is guided by clips that engage the tray's flanges (Figure 1). The tray and plate are then pulled out of the ground as a unit, without vibration. Friction keeps most of the sample in place during this extraction. For further details, see Japan patent 2,934,641 and U.S. patent 6,009,958.

In Japan, a standard geoslicer measures 4 m by 0.4 m by 0.1 m. Wider models have been driven across fault ruptures, and slices 9 -m long have been collected in sheetpile [*Haraguchi et al.*, 1998].

We used sheetpile 9.14 m by 0.55 m by 0.15 m (Figure 1). A 2800-kg hammer, suspended from a crane on a barge, drove the sheetpile and shutter plate at vibrations close to 25 Hz. Each drive lasted a minute or so. The crane then extracted the sampler and its contents, using over 10 t of pull.

Peels

Each sediment slice collected by the geoslicer was enhanced and archived as a full-sized

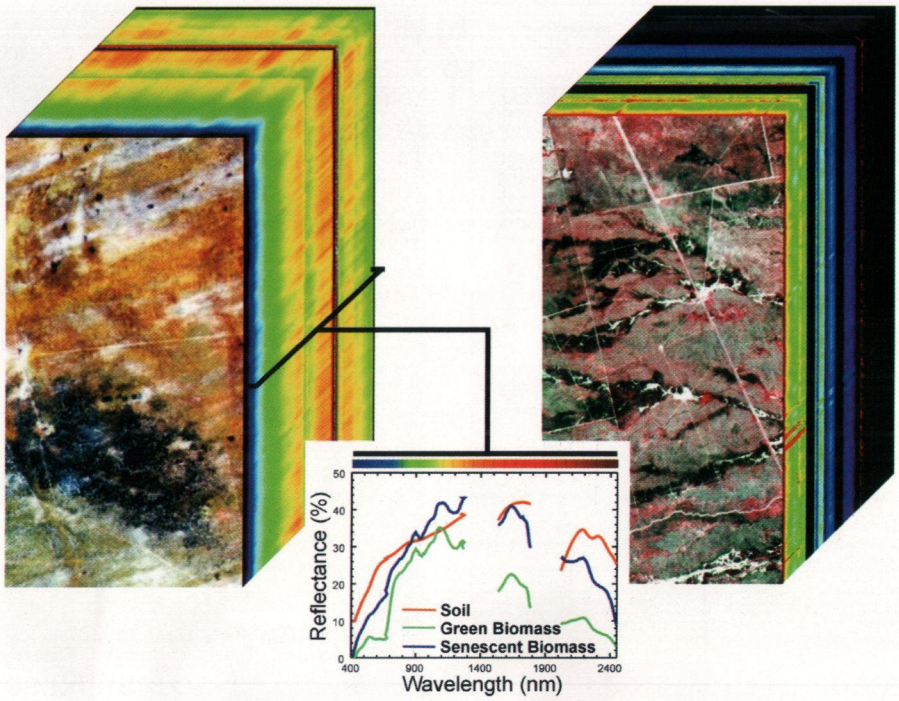

Fig. 1. Imaging spectrometers gather upwelling Earth radiance information in three-dimensional data "cubes," such as in this NASA Airborne Visible and Infrared Imaging Spectrometer (AVIRIS) image of the Jornada LTER arid land research site in New Mexico (left), and this EO-1 Hyperion image of the Ñacuñán Biosphere Reserve, central Argentina (right). The images contain a third spectroscopic dimension that provides quantitative information on the physical and chemical properties of live and senescent vegetation and soils. Example spectra of surface materials demonstrating this third dimension are shown in the graph inset.

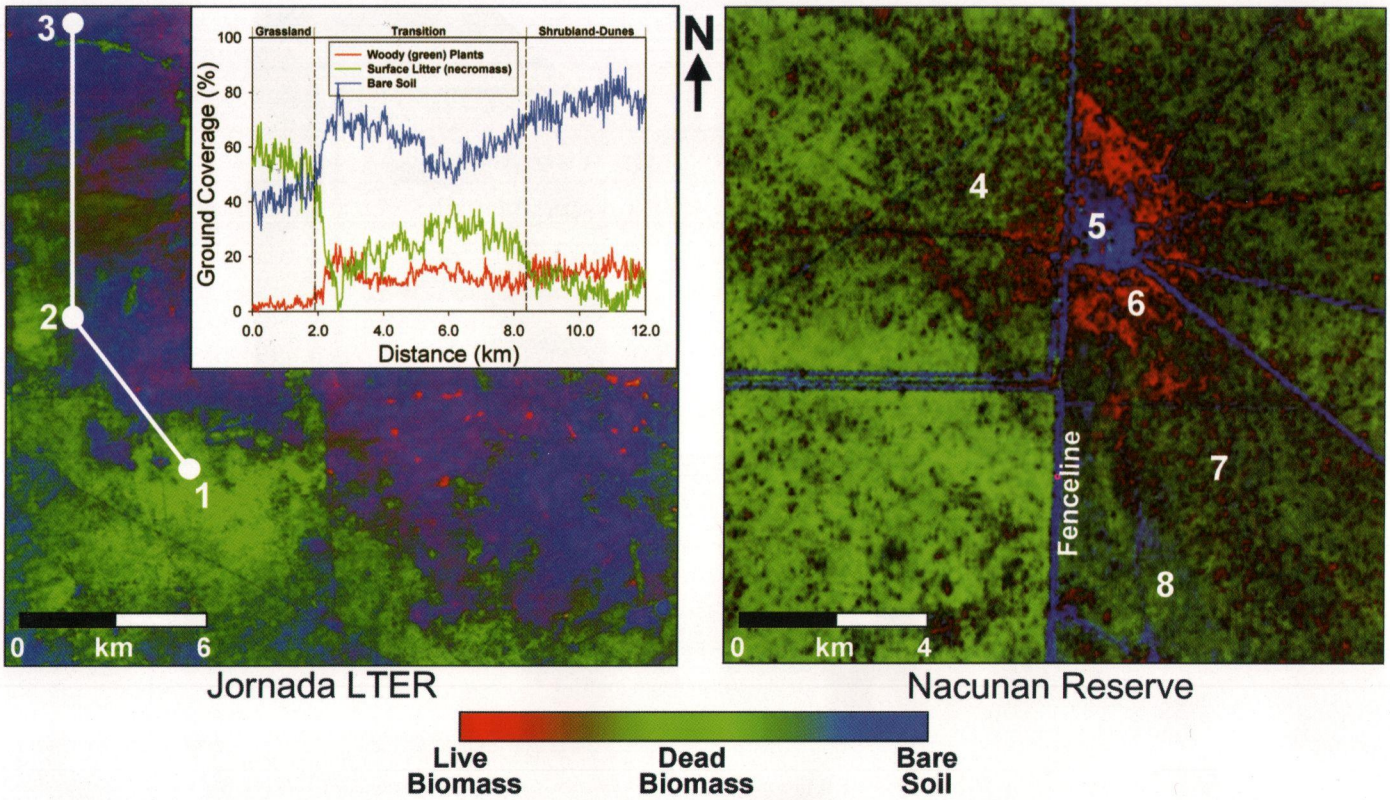

Fig. 3. AVIRIS imagery of the Jornada LTER site (a) and the Ñacuñán Biosphere Reserve (b) is interpreted using physical-spectroscopic models of the land surface. These models are used to estimate fractional cover and biomass of live vegetation and senescent plant materials as well as bare soil cover and geochemistry. The Jornada image contains grasslands (1) that have been converted to shrublands (3) as well as large expanses of transition zone (2) through documented processes of land degradation and desertification. The Ñacuñán image shows the reserve to the left of the center fence line containing areas of mixed live and senescent vegetation with little bare soil (4). To the right of the fence, a cattle ranch (5) is surrounded by thick green, woody vegetation (6) that transitions into areas of low senescent biomass (7) and further to regions of high bare soil cover (8).